Ground and excited state energy trend in InAs/InGaAs quantum dots monitored by scanning photoluminescence spectroscopy

T. V. Torchynska
SEPI–National Polytechnic Institute, Mexico D.F. 07738, Mexico

M. Dybiec and S. Ostapenko
Nanomaterials and Nanomanufacturing Research Center, University of South Florida, 4202 East Fowler Avenue, Tampa, Florida 33620, USA

(Received 11 June 2005; revised manuscript received 29 August 2005; published 29 November 2005)

This paper presents a temperature-dependent scanning photoluminescence spectroscopic study of the ground and excited states on InAs quantum dots (QDs) inserted into $In_{0.15}Ga_{0.85}As/GaAs$ quantum wells. It is shown that structures exhibit a long-range spatial variation of the QD electronic states across the wafer. The observed trend of the ground state energy is attributed to the QD size variation and applied to explore multiple excited state energy shift versus ground state energy. Experimental results are compared with the electronic energy level dependence versus QD size predicted theoretically earlier on the basis of the eight-band $\mathbf{k}\cdot\mathbf{p}$ approximation.

DOI: 10.1103/PhysRevB.72.195341 PACS number(s): 78.67.−n, 78.30.−j, 78.55.−m

I. INTRODUCTION

InAs/GaAs structures with self-assembled InAs quantum dots (QD) have been investigated intensively during the last decade due to their wide device application in optoelectronics.[1,2] Nanometer scaled confinement of electrons in InAs quantum dots (QD) determines the optoelectronic device parameters. This confinement strongly depends on the shape, size, and strain field of a single QD. For basic physics and for creation of optimized devices it is critical to better understand the QD electronic structure which controls its physical parameters. Despite the amount of research done in these areas, the effects of QD size and shape on their energy potential and corresponding electronic levels are not well understood. To our knowledge, the reverse task, to access the QD confining potential on the basis of analyses of QD multiple excited states, has been discussed less often in the literature.

The study of the electronic level structure in Stranski-Krastanow QDs is even more complicated due to a noticeable 7% lattice mismatch between InAs and GaAs layers which produce high strain/stress fields. The strain and quantum confinement create the exciton ground state in InAs QDs with optical transition energy of 0.95–1.10 eV even though the band gap of InAs is only 0.418 eV. Different theoretical assumptions lead to models of the electronic structure in InAs self-assembled QDs. Historically, the first calculations of the electronic structure in QDs were carried out using the effective-mass approximation with parabolic bands[3–6] for spherical,[7] cylindrical,[3,4] or pyramid[5,6] -shaped QDs. The role of strain was accounted for by assuming biaxial strain over the entire dot area for small QD base angles[4] or using elastic continuum theory.[7] These calculations predicted one[6] or two[5] confined electronic levels and the set of confined hole levels in QDs.

More sophisticated calculations were performed later using the perturbation effective-mass approaches,[8] eight-band $\mathbf{k}\cdot\mathbf{p}$ theory,[9–11] or empirical pseudopotential theory.[12] These approaches predicted several electron states for QDs with the size $b \geqslant 10$ nm, but different predictions as to the number and energies of the hole levels. It was shown that the eight-band $\mathbf{k}\cdot\mathbf{p}$ model includes many parameters whose values are not accurately known, but can significantly influence the results.[13] The shortcomings found in the $\mathbf{k}\cdot\mathbf{p}$ calculations included a reduced splitting of the electron p states, an incorrect in-plane polarization ratio for electron-hole dipole transitions, as well as over confinement of both electron and hole states resulting in a band-gap error.[11] The latter stimulated the attempt of joint application of the direct digitalization pseudopotential method to determine the pseudopotential $\mathbf{k}\cdot\mathbf{p}$ parameters, which then can be used in eight-band $\mathbf{k}\cdot\mathbf{p}$ calculation for their improvement.[11] Another improvement of the eight-band $\mathbf{k}\cdot\mathbf{p}$ calculations on QD electronic structures was connected with piezoelectric effects, which affect QD's optical properties.[1,2,10] But even with this improved eight-band $\mathbf{k}\cdot\mathbf{p}$ approach, the meaningful interpretations of optical transitions in QDs is still pending.

At the same time, for theoretical model corrections and specifying assumptions, existing experimental results are not sufficient. As a rule, a comparison of optical transitions with theoretically predicted energies was carried out on the basis of particular results for some definite size and shape of QDs created in different laboratories.[5–12] The latter does not allow the investigation of the trend of electronic (hole) state energy versus monotonic changes of the QD parameters.

A promising method to study the quantum dot electronic state energy trend in InAs/InGaAs quantum dot structures is photoluminescence (PL) scanning spectroscopy. The light beam focused into a 100–200 μm spot at a sufficiently high excitation density of a few kW/cm^2 is able to generate a high concentration of the photocarriers to saturate the ground state (GS) and to fill the excited states (ES) in a QD ensemble at the typical dot surface density of $(3.0–5.5)\times 10^{10}$ cm^{-2}. In this case, the long-range variation of the QD ensemble pa-

rameters can be studied by the PL scanning spectroscopy. The latter allows investigation of general features of the GS and ES energy trends in QDs. This information could be useful for restoring the shape of the dot confinement potential and for corrections of theoretical models of the QD electronic structure.

This paper presents a temperature-dependent scanning photoluminescence spectroscopic study of the ground and excited states on InAs quantum dots (QDs) embedded into $In_{0.15}Ga_{0.85}As/GaAs$ quantum wells (QWs). First, we will show that investigated structures are characterized by a long-range variation of the GS energy levels apparently due to variation of QD sizes in a dot ensemble across the wafer. Second, we will discuss the multi-ES energy variation trend in dependence on the GS energy position exhibiting the QD size effect. Finally, we compare our experimental results with the electronic energy level trend versus QD size predicted by the eight-band $\mathbf{k}\cdot\mathbf{p}$ approximation.[10]

II. EXPERIMENTAL DETAILS

A. Sample preparation

The solid-source molecular-beam epitaxy (MBE) in a V80H reactor was used to grow the waveguide laser structures consisting of three layers of InAs self-organized QDs inserted into $In_{0.15}Ga_{0.85}As/GaAs$ quantum wells (QWs). In the center of the waveguide, an equivalent coverage of 2.4 ML of InAs QDs is confined approximately in the middle of a 9 nm $In_{0.15}Ga_{0.85}As$ QW. Investigated structures are grown under As-stabilized conditions at four different temperatures: 490 °C (1), 510 °C (2), 525 °C (3), and 535 °C (4), during the deposition of the InAs active regions and InGaAs wells, and at 590–610 °C for the rest of the layers. All layers were grown with the growth rate of 0.30 ML/s, but for the QD formation the process provides deposition of 2.4 ML with the growth rate of 0.053 ML/s. The individual dots are of 14–15 nm in the base size and ~7–8 nm in height. The dot density was determined by AFM observation of the parallel wafer that had not been overgrown by QWs and by cladding layers. The in-plane dot density of QDs changed from 9.1×10^{10} to 1.4×10^{10} cm^{-2} when the QD growth temperature increases from 490 to 535 °C. Due to the 16.5 nm GaAs layer (spacer) between the InAs/InGaAs layers, the vertical alignment and electronic coupling of the QDs can be neglected.

B. Experimental setup

The PL spectra were dispersed by a SPEX 500M spectrometer and coupled with a liquid-nitrogen-cooled Ge detector and lock-in amplifier. PL at 12 K was excited by the cw 514.5 nm Ar^+-ion laser line focused down to 200 μm, with power of 300 mW yielding a maximum excitation power density of 1.0 kW/cm^2. Temperature-dependent PL was measured using the closed-cycle cryostat (CCS-450) with a temperature range of 12–300 K. PL spectra at different excitation light power densities were measured using neutral density filters.

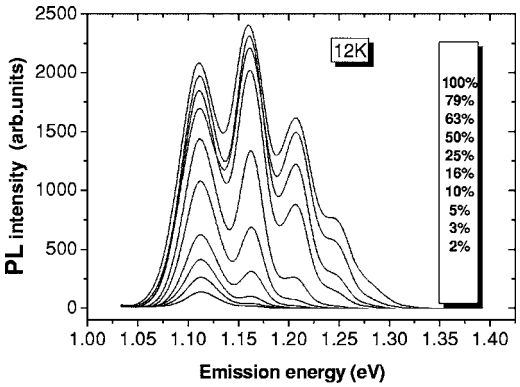

FIG. 1. PL spectra of the QD ensemble measured at different excitation power with the highest one of 1.0 kW/cm^2.

The scanning PL spectroscopy of GSs in QDs was performed at 80 and 300 K, using an intensity modulated 82 Hz solid-state 800 nm IR laser diode with 30 mW average power. The laser beam was focused down to 200 μm in diameter with the excitation power density of ~90 W/cm^2. On the second stage, the ground and multiple excited state PL mapping was performed at 80 K using an Ar^+ laser with light wavelength of 514.5 nm and power up to 200 mW focused down to 200 μm in diameter (excitation power density is up to 650 W/cm^2). Samples were mounted on a PC controlled *X-Y* moving stage. Typical mapping area was a 5 mm $\times$ 15 mm rectangle with the step of 200 μm. PL maps were obtained by the consecutive measurement of the spectra at individual sample spots.

III. EXPERIMENTAL RESULTS

A. Photoluminescence and its temperature dependence

PL spectra measured at different excitation power densities at 12 K are presented in Fig. 1 for the QD structure *N*2 with the QD layer grown at 510 °C. This structure has the highest intensity at 12 K temperature and an excellent resolution of ground and excited PL bands. The spectra reveal a set of PL bands with peak energies of 1.110, 1.160, 1.207, 1.249, and 1.281 eV as can be typically observed on a QD ensemble having a good homogeneity.[14,15] Three former PL bands are well resolved being close to the Gaussian shape. The variation of PL band intensities versus excitation power indicates that the low-energy PL band can be attributed to the ground state (GS) of QDs. The higher-energy PL bands appear at the excitation power density exceeding 100 W/cm^2, indicating the optical transitions via the excited states (1ES-4ES). The deconvolution procedure using Gaussian bands was applied to these spectra, which has shown that the half-width of the three lowest energy PL bands (GS, 1ES, and 2ES) are equal to 39, 31, and 28 meV, respectively. The energy separation between GS and ES bands is not equidistant and equal to 50, 47, 42, and 32 meV, which indicate that studied QDs could not be characterized by a harmonic oscillator potential.[16]

The ground state PL intensity dependence versus temperature for the QD ensemble presented in Fig. 2 has been mea-

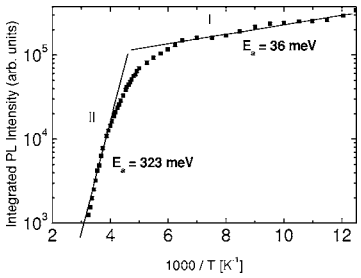

FIG. 2. Ground state PL band intensity dependence vs temperature. Excitation power density was ~650 W/cm^2.

sured at the excitation power of 650 W/cm^2 for the structure *N*2 as well. Two different slopes (I,II) of PL intensity dependence are clearly seen on the temperature curve: the first slope is in the low-temperature range 80–250 K before the main thermal quenching process (II) starts. We estimated the activation energies of these processes by analyzing the temperature dependence of the PL intensity using the Arrhenius plot (Fig. 2). The estimated activation energies are 36 (I) and 323 (II) meV. The excitation light (650 W/cm^2) generates enough photocarriers to fill and even saturate the GS in the QD ensemble at the dot surface density of 5.3×10^{10} cm^{-2} for QD structure *N*2. In this case, we can interpret the PL intensity thermal quenching Ist slope as the carrier thermal escape processes from the QD levels. Taking into account that QDs in this experiment are excited by the light with energy quanta 2.41 eV, which are effectively absorbed in GaAs and wetting layers, the small activation energy 36 meV can also be associated with the thermal carrier escape from wetting layers to the GaAs layer where it is possible for them to recombine via nonradiative channels. The second 323 meV thermal activation energy is larger than the electron-hole binding energy in this type of QD, which typically ranges from 100 to 150 meV.[17,18] Thus, we attribute this high thermal activation energy, 323 meV, to the activation of nonradiative recombination centers.

B. Ground state PL mapping

PL intensity in QD samples measured at 80 and 300 K shows long-range inhomogeneity across the wafer area, which is accompanied by the spectral shift of the PL maximum. We explored this effect in more detail using the spectroscopic PL mapping technique where the PL spectrum is recorded and analyzed at each sample point. As an illustration, we show in Fig. 3(a) the room-temperature PL map measured on a QD structure *N*2 at the energy of 0.99 eV close to the principal PL maximum. Notice the logarithmic scale specified in the contrast bar of Fig. 3(a). White contrast on the map represents higher PL intensity and the dark is the regions of lower intensity. We observe as much as two orders of magnitude variation in the PL intensity signal. This can be seen from the low PL intensity in the central part of the structure to the high PL intensity at the sample periphery area. To establish the origin of such a strong PL inhomogeneity, we performed spectroscopic PL mapping measurements.

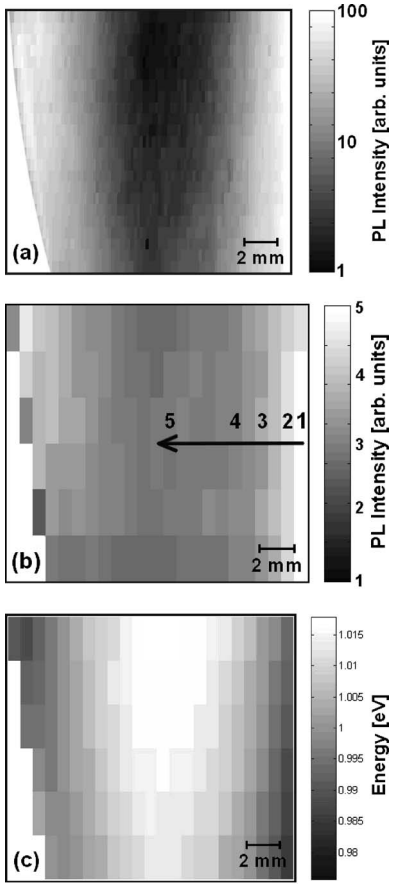

FIG. 3. (a) Map of PL intensity at 0.99 eV (0.25 mm step size, 200 μm excitation spot diameter), (b) map PL intensity at GS max position, and (c) map of peak energy positions (0.5 mm step size) at ~90 W/cm^2 power density. Arrow in (b) corresponds to spectroscopic line scans presented in Fig. 4.

At first the ground state PL scanning spectra were measured at 300 K in high- and low-intensity areas of the QD structure. Low-intensity regions at 300 K are characterized by the "blue" shift of the PL spectrum compared to high intensity areas, as shown in Fig. 4(b). The PL peak position shifts from 0.98 up to 1.02 eV with a threefold decrease of PL intensity. Maps of maximum positions and PL intensities at these maxima were plotted from measured spectra in Figs. 3(b) and 3(c). In correlation with previously described spectra behavior, low-intensity points [dark areas in Fig. 3(b)] are

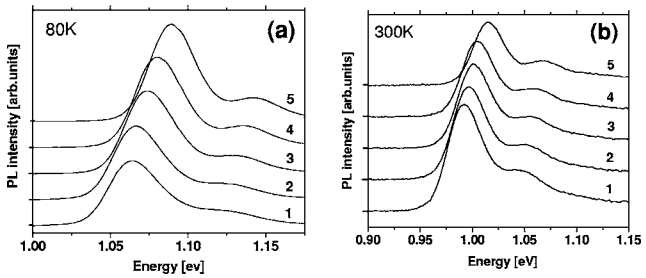

FIG. 4. PL spectra measured at 80 (a) and 300 K (b) at various PL intensity points on QD structure, see Fig. 3(b). (~90 W/cm^2 power intensity).

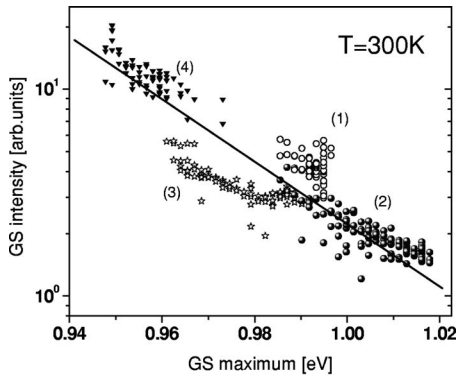

FIG. 5. Ground state PL intensity vs GS maximum position measured at room temperature and 90 W/cm^2 power intensity on four different QD structures grown at different temperatures: (1) 490 °C, (2) 510 °C, (3) 525 °C, and (4) 535 °C.

characterized by a higher energy position of the principal maximum [white areas in Fig. 3(c)]. We observe a clear correlation between PL intensity and PL maximum measured across entire sample areas on four different QD structures $N1-4$ (Fig. 5). Spectroscopic PL mapping was performed across the entire sample's area. In the semilogarithmic plot of the ground state PL intensity versus its GS energy position, this trend can be fitted with a linear dependence as presented in Fig. 5.

We also performed a scanning PL study at 80 K and compared it with room-temperature data along the same line scans. The GS PL peak position shifts at 80 K to the higher energy by 100 meV due to band-gap energy increase [Fig. 4(a)]. Concurrently, a trend of the PL maximum versus PL intensity at 80 K is inverted compared to room-temperature data, i.e., higher intensities correspond to higher PL energy peaks [Fig. 4(a)].

C. Multiple excited states

PL mapping of the ground state and multiple excited states was performed at 80 K at the excitation power density of 650 W/cm^2. In PL spectra measured at high excitation, the three lowest energy PL bands (GS, 1ES, 2ES) are well resolved, which allows us to perform spatially resolved mapping of their peak positions across the sample. Figure 6(a) presents the variation of GS, 1ES, and 2ES energies versus corresponding GS maximum. As one can see, the energy separations are varying across the sample. These separations are 55.5 (GS-1ES) and 45.0 (2ES-1ES) meV for the low-energy GS optical transition at 1.090 eV and it decreases monotonically to 50.9 (GS-1ES) and 31.5 (2ES-1ES) meV for the high-energy GS optical transition at 1.129 eV.

IV. DISCUSSION

A. Ground state PL scanning spectroscopy

We first discuss the long-range GS PL intensity variation across the QD structure which is accompanied by the PL peak shift at 300 K [Figs. 3, 4(b), and 5]. In our earlier paper,[19] we have shown that there are two mechanisms ex-

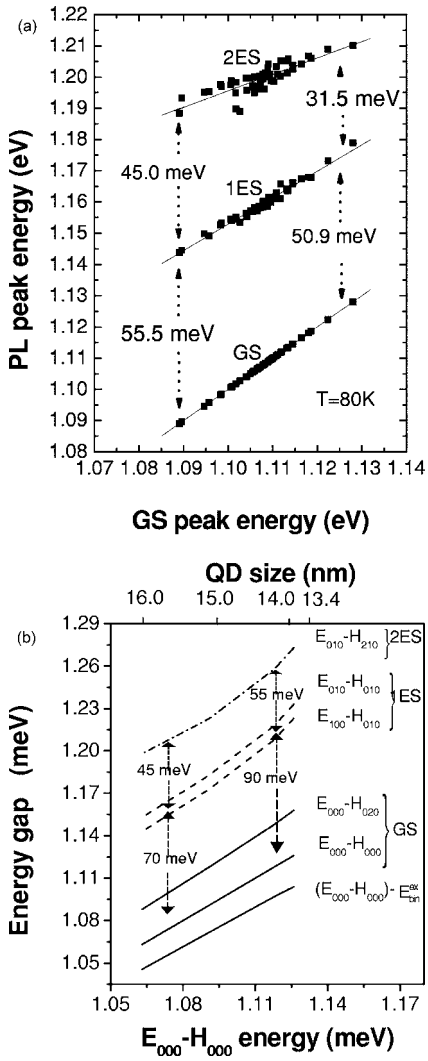

FIG. 6. (a) Experimental peak positions for GS, first, and second ES vs GS peak energy measured at 80 K and excitation power intensity 650 W/cm^2. (b) Theoretically calculated peak positions for GS, first, and second ES vs GS peak energy (or QD size) calculated on the basic of data in Ref. 10.

hibiting PL intensity spatial variation in the InAs QD structures. The first is attributed to inhomogeneous distribution of nonradiative (NR) defects across the QD structures. In this case, scanning PL intensity variation has not been accompanied by the PL spectrum shift. The second mechanism is related to QD parameter changes along the area of high-quality QDs. In the last case, the PL intensity variation is accompanied by a shift of the PL maximum. Our results show that in investigated InAs QD structures the second mechanism of PL inhomogeneity along the structure area takes place.

The ground state PL intensity (I_{PL}) is directly proportional to the excitation light power and the internal quantum efficiency η which can be presented as $\eta=\varpi_R/(\varpi_R+\varpi_{NR})$, where ϖ_R and ϖ_{NR} are radiative recombination (R) and nonradiative recombination (NR) rates, respectively. From the GS PL temperature dependence (Fig. 2) it follows that $\varpi_R \ll \varpi_{NR}$ at 300 K due to thermal quenching of the GS radia-

tive recombination. In this case, the value η can be substituted by the following: $\eta=\varpi_R/\varpi_{NR}$.

For QD ensemble an emission rate is $\varpi_R=\Sigma_{i=1}^{N_D}(f_i^e f_i^p/\tau_R)$, where f_i^e and f_i^p are the occupation probabilities for electrons and holes at ground state levels given by the Fermi-Dirac distribution functions, $f^e, f^p=\{\exp[(E_{n,p}-\mu_{n,p})/kT]+1\}^{-1}$, where $\mu_{n,p}$ are the quasi-Fermi-levels for the conduction and valence bands, respectively, measured from the QD band edges, $E_{n,p}$ are the quantized energy levels of an electron and a hole in the conduction and valence bands of a QD, measured from the QD band edges, N_D is QD density, and τ_R is the electron-hole radiative recombination time.[20] At low excitation light intensity (90 W/cm^2), used during GS PL scanning, which is well below the GS saturation intensity, we can present the occupation probabilities using Maxwell-Boltzmann distribution functions $f^e, f^p=\exp[(-E_{n,p}+\mu_{n,p})/kT]$. Taking into account that excitation light power is not changed during GS PL scanning experiment, we can assume that $\mu_{n,p}$ are constant along the scanning line and the PL intensity variation occurs due to parameters $E_{n,p}$ only. In this case, $f^e\approx\exp(-E_n/kT)$ and $f^p\approx\exp(-E_p/kT)$. The energy levels $E_{n,p}$ can be presented as $E_n=\Delta E_c-E_{\mathrm{loc}}^e$ and $E_p=\Delta E_v-E_{\mathrm{loc}}^p$, where $\Delta E_{c,v}$ are the conduction- and valence-band offsets at the QD-narrow-gap region heteroboundary, measured from the QD band edges, and E_{loc}^p and E_{loc}^e are the binding energies of the electron and hole located at GS levels. We assumed that the values $\Delta E_{c,v}$ and the QD density N_D do not change significantly along the PL scanning line (we will discuss this assumption later) and as a result the variation of $f^{e,p}$ in the PL scanning experiment can be presented as $f^e\approx\exp(E_{\mathrm{loc}}^e/kT)$ and $f^p\approx\exp(E_{\mathrm{loc}}^p/kT)$. In this case, the GS radiative emission rate is changing along the PL scanning line at room temperature as follows:

$$\varpi_R\approx\exp\left(\frac{E_{\mathrm{loc}}^e+E_{\mathrm{loc}}^p}{kT}\right)\approx\exp\left(\frac{E_{\mathrm{GS}}^{\mathrm{InGaAs}}-E_{\mathrm{GS}}^{\mathrm{QD}}}{kT}\right)\approx\exp\frac{-E_{\mathrm{GS}}^{\mathrm{QD}}}{kT}$$
$$\approx\exp\frac{-(h\upsilon_{\mathrm{max}}^{\mathrm{GS}}+E_{\mathrm{bin}}^{\mathrm{ex}})}{kT},$$

where $E_{\mathrm{GS}}^{\mathrm{InGaAs}}$ is the energy gap between GS electron-hole levels in the narrow-gap $In_{0.15}Ga_{0.85}As$ layer and $E_{\mathrm{GS}}^{\mathrm{QD}}$ is the energy gap for GS electron-hole levels in a QD. Here we are taking into account that GS optical transition energy ($h\upsilon_{\mathrm{max}}^{\mathrm{GS}}$) is the difference between $E_{\mathrm{GS}}^{\mathrm{QD}}$ and exciton binding energy $E_{\mathrm{bin}}^{\mathrm{ex}}$ in QDs. Exciton binding energies were computed as the function of QD size using eight-band $\mathbf{k}\cdot\mathbf{p}$ approach and are estimated as 19.5 and 22.5 meV for QDs with the base size 16 and 13.4 nm, respectively.[21] Thus $E_{\mathrm{bin}}^{\mathrm{ex}}$ value changes ($\Delta E_{\mathrm{bin}}^{\mathrm{ex}}\approx 2$ meV) versus QD parameters are small in comparison with GS optical transition energy variation ($h\upsilon_{\mathrm{max}}^{\mathrm{GS}}\approx 1.09-1.25$ eV) [Fig. 6(a)]. Finally, we could obtain scanning PL intensity variation at room temperature very close to the dependence $I_{\mathrm{PL}}\approx\exp(-h\upsilon_{\mathrm{max}}^{\mathrm{GS}}/kT)$, as it demonstrates the fitting line in Fig. 5.

The long-range variation of QD electron and hole localization (binding) energies across the sample area in general can be attributed to the following: (i) QD size changes as a result of inhomogeneous temperature fields across the wafer or InAs layer thickness inhomogeneity during QD growth, and (ii) elastic stress variation across the sample due to layer composition variation. We suppose that the decrease of GS electron-hole binding energies across the scanning area is the result of the long-range variation of an average dot size in the QD ensemble from the periphery toward the sample center. This is exhibited as the "blue" shift of the PL maximum at 300 K [Fig. 4(b)]. This effect leads, at the sample center, to shallower QD localized states (i.e., smallest electron and hole binding energies) and a higher probability of the carrier thermal escape, which reduces their room-temperature PL intensity.

To confirm our assumption and to study this effect in more detail, we performed scanning luminescence at 80 K along the same line scans as for 300 K. At the low-temperature PL scanning measurement, we avoid a process of carrier thermal escape from QDs. As we mentioned above, a trend of the PL maximum versus PL intensity at 80 K is inverted compared to room-temperature data. The twofold rise of PL intensity corresponds to a shift of the PL peak to higher energies from 1.05 up to 1.09 eV [Fig. 4(a)]. We believe that this experiment confirms the assumption of the long-range average size distribution in the QD ensemble. Actually, the GS high-energy PL bands correspond to the smallest QDs, where the electron-hole wave functions strongly overlap, and due to this, the matrix element for optical recombination transitions is relatively large. The opposite holds for GS low-energy PL bands and larger QD sizes. At 80 K, when the carrier thermal escape from QD levels is negligible, this factor governs the high PL intensity of the small-size dots.

B. Ground and multiple excited state PL scanning spectroscopy

The GS and multiple excited state PL scanning spectroscopy was performed at 80 K using higher excitation intensities up to 650 W/cm^2. At high excitation intensity, the QD localized level energies depend on level populations. In this case, the many-particle effects in highly populated QDs are stimulated by exchange/correlation and direct Coulomb contributions should be taken into account.[2] Earlier multiparticle effects were neglected based on the expectation that these contributions no longer exist in the strong confinement limit.[22] Later it was shown that for high populations of InAs/GaAs QDs (with 20 excitons per QD), the GS transitions show a redshift of up to 16 meV and excited state transitions simultaneously experience a blueshift of up to 26 meV.[2]

For quantitative estimation of many-particle effects in our multiple excited state PL mapping experiments, we carried out the measurements of GS and ES peak energy changes versus excitation power in the range of 100–650 W/cm^2. The lowest excitation power density is 100 W/cm^2 due to the fact that at excitation densities smaller than 100 W/cm^2, the ESs have not been detected in the PL spectra. In this experiment, we did not see any redshift of the GS peak with light excitation density in the range of 100–650 W/cm^2 for QDs with GS peak positions in the energy range from

1.09 to 1.129 eV. At the same time, the corresponding 1ES and 2ES peaks show the blueshifts of 4.0–4.2 and 6.5–6.7 meV, respectively.[23]

The analysis of multiple excited state energy trends in InAs/InGaAs QDs versus GS energy (or QD sizes) will be performed in comparison with predicted electron-hole energy gap variations for different electronic sublevels versus QD sizes calculated in Ref. 10 using the eight-band $\mathbf{k}\cdot\mathbf{p}$ approach. Note that theoretical models developed for describing the electronic structure in InAs QDs were elaborated mainly for the InAs/GaAs systems.[1,2,5,6,9–13,18] The InAs/InGaAs QD system is characterized by a lower level of elastic stress due to reduced lattice mismatch at the InAs/$In_{0.15}Ga_{0.85}As$ interface in comparison with InAs/GaAs.[24] Therefore, the electronic structures in InAs QDs for these two systems should be somewhat different.

Another problem is related to the estimation of the QD sizes. As a rule, this estimation is performed using the AFM measurement. Due to the finite size (5 nm) of the AFM tip, the lateral resolution of the AFM method is less than the vertical resolution. This suggests a potential error in our estimation of the QD size in examined InAs/InGaAs structures. As a result, we can only make a qualitative comparison of experimental and theoretical results.

For modeling of GS and 1ES, 2ES optical transitions in InAs QDs, we used the theoretically calculated results obtained via the eight-band $\mathbf{k}\cdot\mathbf{p}$ approach in Ref. 10. Electron-hole state energies presented in Ref. 10 for different sized QDs ranged between 13.4 and 16 nm, close to the size estimated by AFM in examined InAs/InGaAs QDs. On the basis of theoretical calculations of linear absorption spectra for InAs pyramid QDs with the size of 13.6 nm in Ref. 10, the GS PL band is attributed to the superposition of the E_{000}-H_{000} and E_{000}-H_{020} optical transitions. The energy difference between these two transitions is 25–27 meV.[10] It is clear that these two transitions cannot be resolved in our experimental PL spectra with the GS PL band half-width of 38–39 meV.

The 1ES PL band is assigned in Ref. 10 to the superposition of E_{100}-H_{010} and E_{010}-H_{010} optical transitions. The energy difference between these two transitions is 10–12 meV.[10] Thus these two transitions cannot be resolved in our experimental PL spectra as well, because the 1ES PL band half-width is 31 meV. Finally, the 2ES PL band is attributed to the E_{010}-H_{210} optical transition.[10]

Figure 6(b) presents the numerically calculated energy gaps between E_{000}-H_{000}, E_{000}-H_{020}, E_{100}-H_{010}, E_{010}-H_{010}, and E_{010}-H_{210} electron-hole energy levels in InAs QDs versus QD sizes based on the theoretical results of Ref. 10. For further comparison, it is necessary to correct presented electron-hole energy gaps taking into account exciton binding energies for different QD states and sizes. It is known that Coulomb effects are reduced linearly with the increase of the QD size, whereas quantum effects are reduced quadratically. As a result, the GS and ES optical transition energies should increase with decreasing of QD size more slowly than predicted by poor quantum effects. Ground state exciton binding energies were computed in the Hartree approximation using eight-band solutions for both electrons and holes in the QDs with the size 10–18 nm in Ref. 21 or 10.2–20.4 nm in Ref. 10. It was shown that the exciton binding energy increases with decreasing InAs island sizes: the values 19.5 and 22.5 meV for 16 and 13.4 nm QDs[21] or 15.6 and 21.7 meV for 17 and 13.6 nm QDs[10] have been obtained. Thus, with decreasing of the QD size in the range of 16.0–13.4 nm, which is interesting for us in this work, the ground state exciton binding energy should increase by 3–4 meV. The GS transition E_{000}-H_{000} corrected on exciton binding energies for different QD sizes is presented in Fig. 6(b) as well.

Finally, let us compare the main features of experimental and theoretical results presented in Figs. 6(a) and 6(b). As one can see in Fig. 6(a), the energy separation between 1ES and GS PL bands is higher in comparison to the 2ES-1ES value. The theoretically predicted energy difference for 1ES-GS optical transitions is higher than for 2ES-1ES as well. Therefore, we can see correlation between experimental and theoretical results.

But with decreasing QD sizes, the level separation is changed in opposite directions for experimental and theoretical curves. As one can see in Fig. 6(a), the experimental values of energy differences for 1ES-GS and 2ES-1ES PL bands decrease with GS energy increasing (smaller QD): from 55.5 to 50.9 meV and from 45.0 to 31.5 meV, respectively. If we take into account many-particle effects, mentioned above for 1ES and 2ES, this decrease of sublevel energy difference in our experimental case will be even stronger.

Theoretically predicted values of energy spacing increase essentially with QD size decreasing [Fig. 6(b)]: from 60–80 meV up to 70–100 meV for 1ES-GS levels and from 40–50 meV up to 55 meV for 2ES-1ES levels. Unfortunately, we could not find the information concerning the theoretically calculated exciton binding energies for excited states (1ES, 2ES) in different sized QDs. In Ref. 25, it was mentioned that strongly interacting and correlated electrons and holes in QDs can be understood in terms of a gas of weakly interacting excitons and biexcitons. In this case, it is possible to assume that exciton binding energies for excited states in QDs have the same ordering as for GS. Thus, we can conclude that GS and ES optical transition energies should increase with decreasing QD size more slowly than predicted by quantum effect theory.

Note that our experimental results connect with some average GS and ES optical transition energies in the QD ensemble. In this case, the absorption coefficient needs to be presented as the multiplication of the coefficient for a single QD on the distribution function for QD sizes in the ensemble. As was shown in Ref. 26, for example for the Lifshitz-Slezov distribution function of the spherical QDs, the shift of the GS exciton line energy with the QD size in the ensemble should be 0.67 times smaller than the theoretically predicted one for single QDs.

But the main reason for different electron-hole energy trends versus GS energy (QD sizes) for experimental and theoretical results may be related to the different shape of confined potential and its changes with QD sizes in investigated QDs in comparison with theory. Nonequidistant energy spacing between GS and ES indicates that the harmonic-oscillator model is not applicable in studied QDs. As we

have shown in Ref. 16, the formation of ES energy levels in QDs, apparently, due to the nonparabolic shape of the well profile is nonharmonic.

Note, we made the assumption above that the density of QDs along the scanning line on the wafer does not change essentially. We considered the change of the radiative recombination rate due to the variation of electron (hole) binding energy as the main reason of PL intensity variation. Actually, as was shown in Ref. 27 at the AFM investigation of the same type of uncapped InAs QDs grown on the $In_{0.15}Ga_{0.85}As$ layer, the density of QDs changed from 1.1×10^{11} up to 1.4×10^{10} cm^{-2} when the QD growth temperature increases from 470 to 535 °C. For wafers prepared at definite temperatures, such as discussed in our case, the density of QDs across the wafer changes not more than on 50%. So, it is really not an essential variation in comparison with the observed threefold or fourfold magnitude variation in the PL intensity signal at room temperature (Fig. 5).

V. CONCLUSIONS

The photoluminescence at 12 K and scanning PL spectroscopy at 80 and 300 K of the ground and multiple excited states in InAs/InGaAs QDs have been investigated. It was shown that examined QD structures are characterized by the long-range variation of QD parameters across the sample, apparently, due to variation of the QD size. This fact gives the possibility for investigating the QD excited state energy trends versus average ground state energy variations (or QD sizes) in the QD ensemble. We compared our experimental results with the electronic energy level trend versus QD sizes predicted on the basis of the eight-band $\mathbf{k}\cdot\mathbf{p}$ approach.

ACKNOWLEDGMENTS

The authors thank Dr. Andreas Stintz from the Center of High Technology Materials at the University of New Mexico for growing the studded InAs quantum dot wafers and Professor Dr. P. G. Eliseev for fruitful discussions. The work was supported by CONACYT (Project No. N 42436-Y), as well as by National Science Foundation Grant No. DMI-0218967 and CGPI-IPN Mexico.

[1] D. Bimberg, M. Grundman, and N. N. Ledentsov, *Quantum Dot Heterostructures* (Wiley & Sons, New York, 2001), p. 328.
[2] *Nano-Electronics*, edited by M. Grundmann (Springer, Berlin, 2002), p. 442.
[3] L. Jacak, P. Hawrylak, and A. Wojs, *Quantum Dots* (Springer, Berlin, 1998), p. 176.
[4] J. Y. Marzin and G. Bastard, Solid State Commun. **92**, 437 (1994).
[5] M. A. Cusack, P. R. Briddon, and M. Jaros, Phys. Rev. B **56**, 4047 (1996).
[6] M. Grundmann, O. Stier, and D. Bimberg, Phys. Rev. B **52**, 11969 (1995).
[7] D. B. Tran Thoai, Y. Z. Hu, and S. W. Koch, Phys. Rev. B **42**, 11261 (1990).
[8] L. R. C. Fonseca, J. L. Jimenez, J. P. Leburton, and R. M. Martin, Phys. Rev. B **57**, 4017 (1998).
[9] H. Jiang and J. Singh, Phys. Rev. B **56**, 4696 (1997).
[10] O. Stier, M. Grundmann, and D. Bimberg, Phys. Rev. B **59**, 5688 (1999).
[11] L. W. Wang, A. J. Williamson, A. Zunger, H. Jiang, and J. Singh, Appl. Phys. Lett. **76**, 339 (2000).
[12] A. Zunger, MRS Bull. **23**, 35 (1998).
[13] C. Pryor, Phys. Rev. B **60**, 2869 (1999).
[14] S. Fafard, Appl. Phys. Lett. **76**, 2707 (2000).
[15] G. Park, O. B. Shchekin, D. L. Huffaker, and D. G. Deppe, Appl. Phys. Lett. **73**, 3351 (1998).
[16] P. G. Eliseev, D. P. Popescu, T. V. Torchynska, A. Stintz, and K. J. Malloy, Proc. SPIE **5349** (2004).
[17] T. V. Torchynska, J. L. Casas Espinola, P. G. Eliseev, A. Stintz, K. J. Malloy, and R. Pena Sierra, Phys. Status Solidi A **195**, 209 (2003).
[18] T. V. Torchynska, J. L. Casas Espinola, E. Velasquez Losada, P. G. Eliseev, A. Stintz, K. J. Malloy, and R. Pena Sierra, Surf. Sci. **532–535**, 848 (2003).
[19] M. Dybiec, S. Ostapenko, T. V. Torchynska, and E. Velazquez Lozada, Appl. Phys. Lett. **84**, 5165 (2004).
[20] L. V. Asryan and R. A. Suris, Semicond. Sci. Technol. **11**, 554 (1996).
[21] C. Pryor, Phys. Rev. B **57**, 7190 (1998).
[22] S. Schmitt-Rink, D. A. B. Miller, and D. S. Chemla, Phys. Rev. B **35**, 8113 (1987).
[23] T. V. Torchynska, H. M. Alfaro Lopez, J. L. Casas Espinola, P. G. Eliseev, A. Stintz, K. J. Malloy, and R. Pena Sierra, Microelectron. J. **36**, 186 (2005).
[24] V. M. Ustinov, N. A. Maleev, A. E. Shukov, A. R. Kovsh, A. Yu. Egorov, A. V. Lunev, B. V. Volovik, I. L. Krestnikov, Yu. G. Musikhin, N. A. Bert, P. S. Kopev, Zh. I. Alferov, N. N. Ledentsov, and D. Bimberg, Appl. Phys. Lett. **74**, 2815 (1999).
[25] A. Wojs and P. Hawrylak, Solid State Commun. **100**, 487 (1996).
[26] Al. Efros and A. Efros, Sov. Phys. Semicond. **16**, 772 (1982).
[27] A. Stintz, G. T. Liu, L. Gray, R. Spillers, S. M. Delgado, and K. J. Malloy, J. Vac. Sci. Technol. B **18**(3), 1496 (2000).